

Hydrophobization effect on wetting, drying and salt crystallization in porous materials

Noushine Shahidzadeh

University of Amsterdam, Institute of Physics, Science Park 904, 1098XH Amsterdam, The Netherlands.

SUMMARY: We discuss the major role played by both the wetting properties of the porous material and the boundary conditions on the drying process. For hydrophobic materials, it will be shown how under some circumstances the evaporation rate becomes lower in the presence of an air flow over the surface than without an air flow, which at first sight seems counterintuitive. Furthermore, how entrapped sodium chloride solution can reach a high supersaturation before crystallization, contrary to what is commonly assumed for this salt. A consequence of such a high concentration is the very rapid growth of a single skeletal (Hopper) crystal, which can lead to damage.

KEY-WORDS: hydrophobic surface, sandstone, crystallization, sodium chloride, evaporation.

INTRODUCTION

Porous materials such as rocks, bricks, concrete, cement and wood when in contact with the atmosphere are continuously subjected to imbibition–drying cycles which seriously affect their durability, in particular because particle or ion transport may lead to chemical alterations of the structure [1-5]. The use of a wide range of hydrophobic surface treatments ‘*water-repellent products*’ in civil engineering, in the building conservation industry and in soils suggests that the wetting properties of the matrix plays a key role in water transfer through porous media. Mostly, the aim of such water-repellent treatments is to create a protective layer, to reduce the weathering rate of natural building stones and to improve the mechanical properties of the weakened materials [6-8].

In soil mechanics, the use of hydrophobic sand significantly decreases the amount of water required for plant irrigation in desertic regions and encourages plant growth in arid climates. In fact, degradation and desertification of soils due to sodium chloride is a major physiological threat to ecosystems [9,10].

In civil engineering, hydrophobic treatments can prevent water from imbibing the porous medium, thus limiting the damage that can result from its presence. Pertinent examples of such damage are salt weathering during drying (displacement of ionic solutions towards the surface and their subsequent crystallization when the water evaporates) or frost damage due to the freezing of water within the porous medium [11]. The efficiency of consolidant and water repellent treatments strongly depends on their impregnation depth which will in turn affect the wetting properties of the porous materials and change the flow of the liquid within the porous matrix [12-15].

One of the important observations from previous research on the topic is that hydrophobic treatments can lead to the formation of entrapped liquid pockets in a porous network, since it prevents a water-continuous phase to reach the surface of the porous media. All these considerations call for a better understanding of the wetting characteristics effect of the liquid on/in the porous medium as well as on the drying speed of the wet material material and the subsequent kinetics of crystallization in the case of salt solution.

This paper reports our drying experiments on model porous media with well controlled wetting properties of the solid. In addition, the boundary conditions were varied by studying the effect of the presence (or absence) of an air flow at the evaporating surface. For hydrophobic materials, it was found that under some circumstances the evaporation rate becomes lower in the presence of an air flow over the surface than without an air flow, which at first sight seems counterintuitive.

Subsequently, experiments on the evaporation of salt solutions trapped inside a porous medium for different degrees of confinement. i.e., pore sizes, are presented. The high supersolubility achieved before crystallization in these experiments shows that, contrary to what is commonly assumed for this salt, an elevated supersaturation can be reached before crystal growth occurs. These findings have far-reaching implications for the widespread consequences of salt crystallization since the salt weathering of rocks, stones, and monuments is related to the crystallization pressure, which is directly dictated by the supersaturation and the importance of which is expected to increase in the future due to global climate change.

EXPERIMENTAL

Evaporation in hydrophobic and hydrophilic porous media

The particular problem we aim to address is the relative importance of different transport mechanisms in the liquid and vapor phases during the drying process. To assess the role of capillarity on the transport of the liquid phase, the wettability of the porous media were modified. To investigate the role of the transport mechanism in the vapor phase, slow and fast drying experiments were carried out by either having an air flow over the surface or carefully avoiding air movement [16]. All experiments reported here were done for a given constant relative humidity (RH) $46\pm 2\%$ and temperature 21°C (T).

Model porous media consisting of hydrophilic or hydrophobic glass beads of $240\text{--}320\text{ }\mu\text{m}$ diameter range were used. Hydrophobic beads were obtained by silanization with a fluorinated silane solution (Evonik Dynasylan F8261). The contact angles (advancing and receding) of water, determined from micro-photographs of the bead in contact with a droplet over a flat surface, were $\theta_a = 11\pm 5^\circ$ and $\theta_r \sim 0^\circ$ for hydrophilic beads and $\theta_a = 88\pm 5^\circ$ and $\theta_r = 84\pm 5^\circ$ for hydrophobic ones [17]. The porous media were obtained by filling a glass column (porosity, $p \approx 35\%$) with an automated packing system (diameter 3 cm, height 3 cm). Since the liquid retracts itself from the porous medium during drying.

The water saturated porous media were dried from the top surface in a controlled atmosphere chamber in the absence or in the presence of an air flow (0.2 m s^{-1}) at this surface. The weight of the sample was measured over time on an automated balance with a precision of ($\pm 0.001\text{ g}$). The saturation profiles during drying were obtained by measuring the absorption of gamma-ray radiation by the water in the sample.

For hydrophilic beads saturated with pure water and in presence of an air flow, the typical drying behavior is a constant drying rate ($\sim 0.12 \text{ g h}^{-1}$) followed by a much slower drying that sets in at a very late stage, almost at complete desaturation (Figure 1). In the absence of an air flow a constant drying rate (CRP, constant rate period) is also achieved but it is about three times lower ($\sim 0.037 \text{ g.h}^{-1}$). The critical saturation at which the CRP ends, generally referred to as critical moisture content (about 7%), turns out to be independent of the boundary conditions. The CRP is clearly associated with a homogeneous desaturation of the sample, i.e., there is no drying front down to very low liquid content, although there may be a slight decrease of the liquid saturation very close to the free surface of the sample (Figure 2(a)).

These results are similar to those obtained by Guillot et al. [18] from MRI measurements on a drying porous rock. Moreover this result is in agreement with the simulations of Yiotis et al. [19] showing that a CRP period is associated with the existence of a continuous liquid film in contact with the free surface of the sample. Yiotis et al. [19] identified that this period effectively corresponds to the CRP, but could not give a definite explanation for the fact that the drying rate remains constant whereas the saturation (water content) decreases on average. One possible explanation is that the evaporation from a partially saturated porous material is similar to that from a sample with a fully wetted free surface. This explanation relies on the theoretical work of Suzuki et al. [20] who showed that the evaporation from a dispersion of liquid patches on a planar solid surface is almost constant as long as the fraction of liquid–gas interface is larger than 10%. However, in a porous material the evaporation from liquid patches below the free surface of the sample must *a priori* also be taken into account. Therefore, it was suggested that the vapour density below this surface rapidly reaches a value close to its maximum, thus limiting evaporation [20].

Several models [19, 20] describing the drying rate from a single pore with a specific shape provide some insight into the basic physical process at the origin of some of our observations: at the local scale of the pore there is a regime for which a liquid film flows along the pore surfaces at a constant rate making it possible to maintain a CRP while vapor transport due to diffusion from the interior of the pore remains negligible.

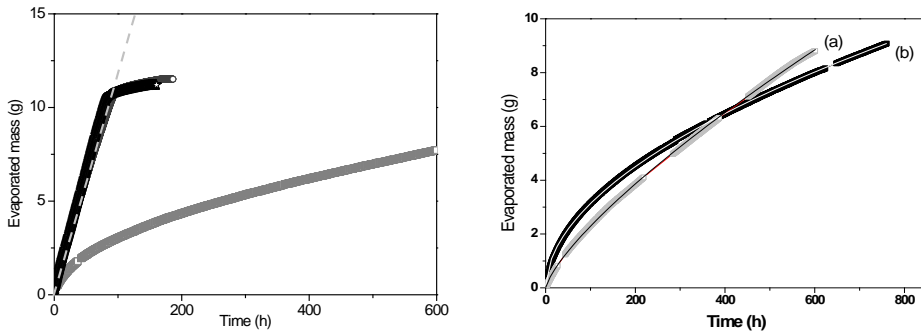


Figure 1. Left: Evaporated mass of liquid as a function of time for homogeneous hydrophilic (circles), hydrophobic (grey squares) porous media in the presence of an air flow on the top surface (0.2 m s^{-1}). Right: Evaporated mass of liquid as a function of time for a hydrophobic porous medium (a) without air flow and (b) in the presence of an air flow on the top surface (0.2 m s^{-1}) [16].

The results for the hydrophobic porous medium are completely different. As can be observed in Fig. 1, the time required to reach a saturation of approximately 25% is about ten times longer for hydrophobic than for hydrophilic beads. Surprisingly, when an air stream is blowing over the sample, the evaporation shows an even smaller drying rate (Figure 1). The saturation profiles (Fig. 2(b)) also differ from those of the hydrophilic porous medium: the saturation decreases to zero close to the free surface, leading to a clear drying front that subsequently propagates into the material, and the drying rate decreases as the square root of time (0.52 ± 0.02). It follows from this, that for the hydrophobic porous medium the capillary forces are not strong enough to ensure liquid transport to the surface at a rate that is comparable to the evaporation rate.

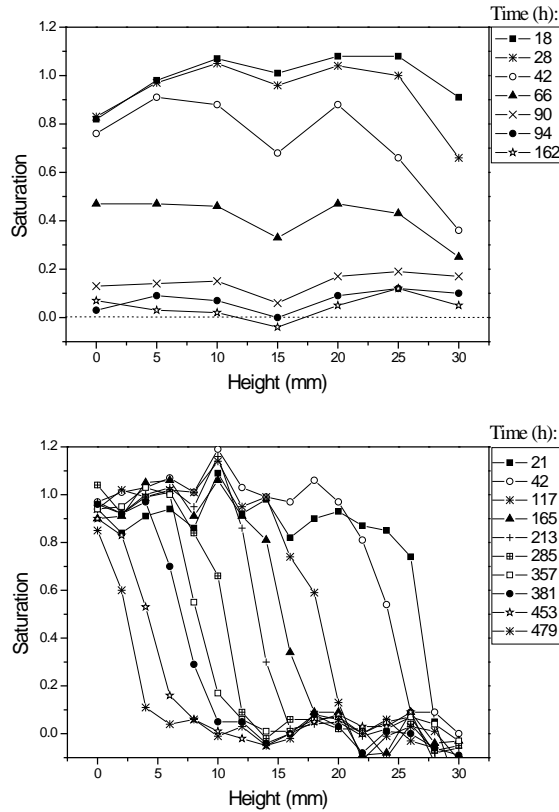


Figure 2. Saturation profiles within the sample in the presence of air flow for: (top) hydrophilic porous media; (bottom) hydrophobic porous media.

This very large difference between hydrophilic and hydrophobic porous media is clearly due to the wetting properties, since all other parameters in our experiment were the same. The capillary rise $2\gamma \cos \theta_a / \rho g r$, in which ρ is the water density, g the gravity and r the typical pore radius ($\sim 40 \mu\text{m}$), is only $\sim 3.5 \text{ cm}$ in the hydrophobic medium while it is $\sim 35 \text{ cm}$ in the hydrophilic one. Moreover, performing the classical Washburn experiments on the rate of capillary rise in our hydrophilic and hydrophobic porous media reveals that the rate of

capillary rise for hydrophobic packing can be 5000 times smaller than that for the hydrophilic ones. Consequently, the observation that the drying front starts at the free surface and subsequently penetrates into the porous medium suggests that it is the speed of capillary transport that is insufficient in hydrophobic media to ensure saturation at the evaporating surface. The evaporation therefore takes place within the porous medium, and the evaporated molecules subsequently diffuse out of the porous material.

In the absence of air flow, the drying dynamics for the hydrophobic matrix are also very different. The evaporated mass as a function of time is no longer linear, but may be fitted by a power law behavior with an exponent 0.75 ± 0.02 , intermediate between that for the hydrophilic beads (CRP, exponent 1) and hydrophobic beads in the presence of air flow at the surface (exponent 0.5, due to diffusion of water vapor through the air within the porous medium). This result suggests that without air flow over the surface, because of wetting heterogeneities in the hydrophobic porous medium, some slow local capillary rise from the deeper regions to the top of the sample may subsist, while the rest of sample dries by diffusion. Over long times, when the moisture content in the sample becomes low, the evaporation via this local capillary rise could become predominant, thus explaining the surprising fact that the total evaporated mass becomes larger when there is no air flow over the top surface, than with it. Although the resolution of our gamma-ray measurement is not sufficient to reach a definitive conclusion, the data obtained for the saturation profiles over time seem to confirm this interpretation: for most of the drying period the porous medium just below the surface remains saturated between 10 and 30% even over long times, in contrast with the result with air flow for which the moisture content is near zero as soon as the drying front has passed.

Evaporation of entrapped salt solution in hydrophobic sandstone

This section discusses the results obtained for the evaporation of a salt solution when trapped by capillary forces in the porous network. To study this, experiments both on micro capillaries and on real sandstone were carried out done using sodium chloride as the salt. Glass microcapillaries with different surface properties were used: hydrophilic (cleaned) and hydrophobic (silanized), as simple model systems for a single pore in a porous medium [22]. The range of capillary sizes (from 20 to 2000 μm) used in the experiment interpolates between bulk evaporation for the largest capillaries and evaporation in pores representative of typical porous media such as natural stones and soils.

To be able to compare the results in capillaries and natural sandstone, the formation of entrapped liquid pockets in the porous network was facilitated by treating the surface of the stone with a water repellent product (by silanization). As discussed in the previous section, the hydrophobic treatment slows down the evaporation, prevents salt from crystallizing at the exterior of the stone, and facilitates the formation of liquid pockets.

The crystallization is induced by evaporation under isothermal conditions ($T = 21 \pm 1$ °C): a known volume V_0 of the NaCl solution ($m_i = 4.9$ mol·kg⁻¹) is introduced into the capillary or the real porous media and placed into a miniature climatic chamber.

The volume change during the evaporation of the solutions inside the microcapillaries is subsequently followed by recording the displacement of the two menisci while simultaneously visualizing the onset of crystal growth in the solution directly with an optical

microscope coupled to a CCD camera. Figure 3 shows the supersaturation at the onset of spontaneous crystal growth for different sizes, shapes, and surface chemistry of the capillaries. From the results of over 100 experiments, a limit of supersaturation of $S \sim 1.6 \pm 0.2$ was found. This is very high compared to the metastability limit reported in the literature for sodium chloride in cooling experiments, $S \sim 1.03$ [23].

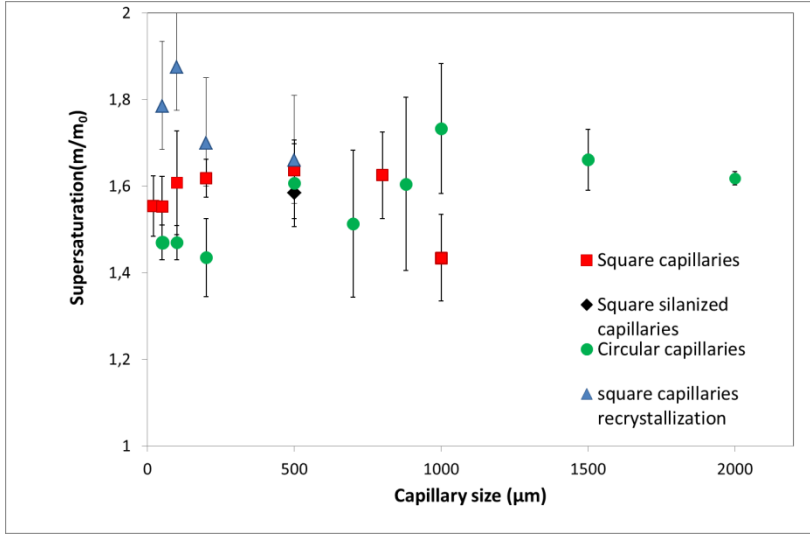


Figure 3. Supersaturation ($S = m/m_0$) of NaCl solutions reached by evaporation at the onset of nucleation and growth (m and m_0 are molalities $\text{mol} \cdot \text{kg}^{-1}$ at the onset of crystallization and at equilibrium respectively for microcapillaries of different sizes, geometries (square and circular), and wetting properties (cleaned and silanized) at $\text{RH} \sim 52 \pm 2\%$.

To investigate whether the supersaturation was well-defined in terms of the NaCl concentration, the Peclet number (Pe), which is a measure of the heterogeneity of the ion distribution, was determined. Pe is defined as the ratio between the convective and the diffusive transport of ions in the solution and it was found to be initially in the order of 1, but decreases to values in the order of 10^{-2} to 10^{-3} at the onset of nucleation [22]. This confirms a homogeneous distribution of ions in the solution and can mainly be attributed to the decrease in evaporation rate, as shown in Fig. 4.

The conclusion is that the saturated salt solutions evaporate for a long period of time without any nucleation and growth of crystals. This implies that the salt concentration in the solution increases; one of the consequences of this is an increase in the liquid-vapor surface tension γ_{lv} of the solution which avoids the formation of a wetting film [24] and the decrease on the saturated vapor concentration above the solution ($c_i/c_{\text{pure water}} = 1 - 0.24 S$). Both these effects lead to a decrease in evaporation rate with time. It is interesting to note in Fig. 4 that, independently of the time necessary to reach it, the crystallization is only observed when a supersaturation of 1.6 is achieved, corresponding to an amount of evaporated water of around 0.5.

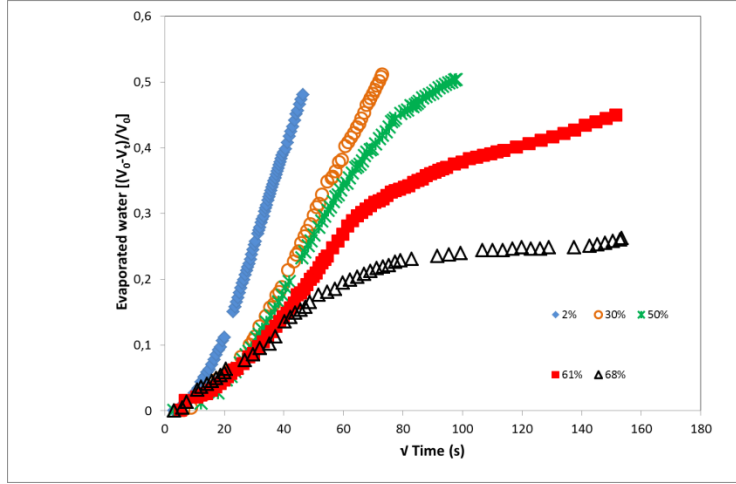


Figure 4. Normalized evaporated water volume as a function of square root of time at different relative humidities until spontaneous crystal growth is observed ($m_i = 4.9 \text{ mol} \cdot \text{kg}^{-1}$, $d = 200 \text{ } \mu\text{m}$ square capillaries) [22].

Surprisingly, at the onset of crystallization only a single crystal nucleus is observed to grow very rapidly forming a hopper shaped (skeletal) crystal (Fig. 5). The growth of the hopper crystals in these experiments happens at a speed that can be up to 10 times that of the growth of a regular cubic crystal under the same conditions. The rapid growth of the hopper crystal is the result of the high supersaturation where secondary nucleation may occur at the corners of the growing primary nuclei, due to the disparity of growth rates between the crystal edges and the crystal faces [25]. It is likely that such fast growth dynamics may provoke damage in porous materials; indeed, the crystallization pressure that is responsible for the damage is known to depend strongly on the supersaturations reached.

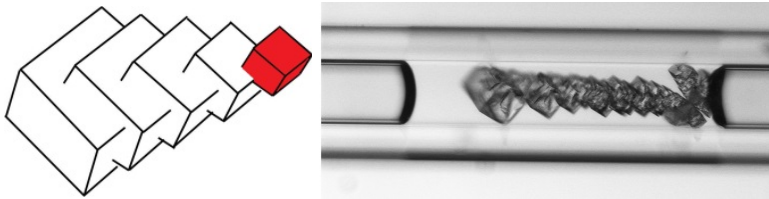


Figure 5. Formation of hopper crystals at onset of crystallization at high supersaturation in a hydrophobized capillary.

Comparisons were made between the NaCl crystal morphologies in microcapillaries at the late stages of drying in water repellent treated porous sandstone (Mešne/Prague sandstone with average pore diameter $d \sim 30 \text{ } \mu\text{m}$ and porosity $\sim 29\%$). After saturation of the stone with the initial salt solution ($m_i = 4.9 \text{ mol} \cdot \text{kg}^{-1}$), the latter is dried under the same environmental conditions as the capillaries. Subsequently, the sample is fractured, and the salt crystal morphology inside the stone is investigated by scanning electron microscopy (SEM).

Figure 6 shows the remarkable similarities between the crystal structures formed in the stone after complete drying and in the capillaries, hopper crystals always formed. Observations on several samples show that these crystals are plentiful in some regions of the stone, and almost absent from others, suggesting that very concentrated residual fluid pockets formed during evaporation. Both these observations indicate for the first time that the liquid forms pockets that can reach high supersaturations before crystallization sets in. This supersaturation seems to be sufficient to provoke weathering. In fact, at $S = 1.6$, the crystallization pressure [26] is about $\Delta P \sim 160$ MPa.

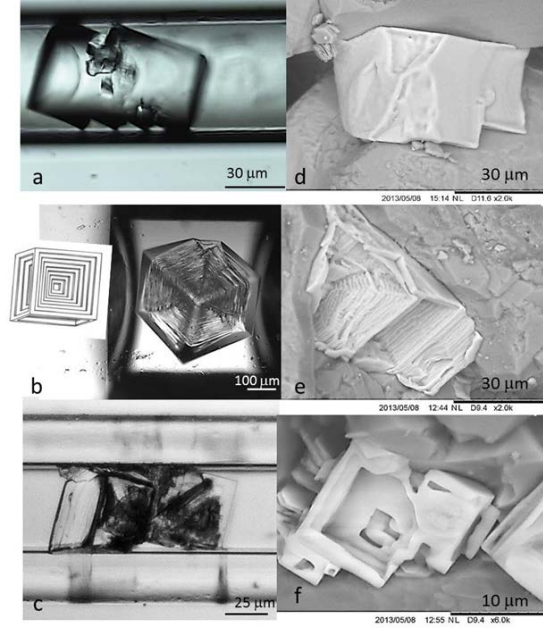


Figure 6. NaCl hopper crystals formed in hydrophobic capillaries (on the left) and on hydrophobic sandstone (on the right) after reaching the supersolubility of $S=m_c/m_s=1.6$.

CONCLUSIONS

The major role played by both the wetting properties of the porous matrix and the boundary conditions (presence or absence of an air flow) on the drying process of porous media has been shown. The rate of evaporation of a hydrophilic porous medium and a hydrophobically treated identical porous structure are very different. In the case of a hydrophobic porous medium the evaporation kinetics is far slower because of the small capillary rise related to the wetting heterogeneities (partially wetted surface). If the evaporating surface is no longer wetted by the liquid (corresponding to a receding drying front), the evaporated molecules have to be transported by a vapor diffusion process through the porous structure. A surprising consequence of the competition between localized capillary rise and diffusion is that over relatively long time periods the evaporation rate can become smaller when an air flow is present than when it is not, because when it is present, the water phase no longer

reaches the surface after the initial drying time during the evaporation process. Consequently, drying becomes governed by vapor diffusion only associated with a receding (dry) front which ultimately favors the formation of liquid pockets in the porous network.

The results obtained from the evaporation of sodium chloride solutions show that the very slow evaporation from such liquid pockets can lead to high supersaturations before crystallization sets in, contrary to what is commonly assumed for this salt. One of the consequences of the high supersaturation reached is the formation of hopper crystals rather than the typical cubic shape, which was also found to occur in experiments conducted on sandstone treated by a water repellent product.

These findings have far-reaching implications for the widespread consequences for salt weathering of rocks, stones, and other porous building materials, where deterioration is related to the crystallization pressure, which in turn is directly dictated by the salt supersaturation. While hydrophobic treatments may prevent the efflorescence of the salt at the surface of the stone, it allows the solution to reach high supersaturations, and consequently the delayed damage is likely to be far worse.

REFERENCES

- [1] SHAHIDZADEH-BONN, N.; J. Desarnaud, F. Bertrand, X. Chateau, D. Bonn. 2010. *Damage in Porous Media due to Salt Crystallization*. Phys. Rev. E. 81:0661101.
- [2] GONCALVES, T. Diaz, V. Brito. 2014. *Alteration kinetics of natural stones due to sodium sulphate crystallization: can reality match experimental simulations?* Environ. Earth. Sci. DOI 10.1007/s12665-014-3085-0.
- [3] LUBELLI, B., R. P. J. Van Hees, H. P. Huinink, C. J. W. P. GROOT. 2006.. *Irreversible Dilation of NaCl contaminated lime-cement Mortar due to Crystallization cycles*. Cement Concrete Res. 36:678-687.
- [4] ESPINOSA-MARZAL, R., G. W. Scherer. 2013. *Impact of in-pore Salt Crystallization on transport properties*. Environ Earth Sci. 69:2657-2669.
- [5] VERAN-TISSOIRES, S., M. Marcoux, M. PRAT. 2012. *Discrete Salt Crystallization at the Surface of a Porous Medium*. Phys.Rev. Lett. 108:054502.
- [6] WHEELER, G. *Alkoxysilanes and the Consolidation of Stone*. 2005. The Getty Conservation Institute, Los Angeles, CA.
- [7] HANSEN, Eric. E. Doehne, J. Fidler, J. Larson, B. Martin, M. Matteini, C. Rodriguez-Navarro, E.S. Pardo, C. Price, Clifford; A. De Tagle, J. M. Teutonico, N. Weiss. 2003. *A review of selected inorganic consolidants and protective treatments for porous calcareous materials*, Reviews in conservation, 4:13-15 .
- [8] DOEHNE, E., C. A. PRICE. *Stone conservation*. 2010. Getty Conservation Institute, Los Angeles, CA.
- [9] SALEM M., W. Al Zayadneh, A. J. Cheruth. 2010. *Water conservation and management with hydrophobic encapsulation of sand*, Water Resources Management, 24:2237-2246.
- [10] WONG, V. N., R. C. Dalal, R. S. Greene. 2008. *Salinity and Sodicity effects on respiration and Biomass of soil*. Biology and Fertility of Soils. 44:943-953.

- [11] JACKSON K. A., B. Chalmers. 1958. *Freezing of Liquids in Porous Media with Special Reference to Frost Heave in Soils*, Journal of Applied Physics 29:1178.
- [12] BRINKER C. J., G. W. SCHERER 1990. *The Physics and Chemistry of sol-Gel processing*, Academic Press Inc., San Diego, CA.
- [13] BRUS, J., P. Kotlik. 1996 *Consolidation of stone by mixtures of alkoxysilane and acrylic polymer*, Studies in Conservation, 41:109–119.
- [14] MOSQUERA, M. J., J. Pozo. 2003. *Stress During Drying of Two Stone Consolidants Applied in Monumental Conservation*, Journal of Sol-Gel Science and Technology 26: 1227-1231.
- [15] ILLESCAS, J. F., M. J. Mosquera. 2011. *Surfactant-Synthesized PDMS/Silica Nanomaterials Improve, Robustness and Stain Resistance of Carbonate Stone*, Journal of Physical Chemistry C, 115:14624–14634.
- [16] SHAHIDZADEH-BONN, N., A. Azouni, P. Coussot. 2007. *Effect of wetting properties on the kinetics of drying of porous media*, Journal of Physics: Condensed Matter 19:112101.
- [17] SHAHIDZADEH-BONN, N., A. Tournié, S. Bichon, P. Vié, F. Bertrand, S. Rodts, P. faure, A. Azouni. 2004. *Effect of wetting on the dynamics of drainage in porous media*, Transport in Porous Media 56:209-224.
- [18] GUILLOT G., A. Trokiner, L. Darasse, H. Saint-Jalmes. 1989. *Drying of a porous Rock Monitored by NMR Imaging*, Journal of Applied Physics **D**, 22:1646-1649.
- [19] YIOTIS, A. G.; A. K. Stubos, A. G., Boudouvis, I. N. Tsimpanogiannis, Y. C. Yortsos. 2005. *Pore-Network Modeling of Isothermal Drying in Porous Media*, Transport in Porous Media 5:63–86.
- [20] SUZUKI, M., S. Maeda. 1968. *On the mechanism of drying of granulars beds*, Journal of Chemical Engineering of Japan, 1:26-31.
- [21] PRAT, M, F. Bouleux. 1999. *Drying of capillary porous media with stabilized front in two dimensions*, Physical Review **E** 60:5647
- [22] DESARNAUD, J.; H. Derluyn, J. Carmeliet, D. Bonn, N. Shahidzadeh. 2014. *Metastability Limit for the Nucleation of NaCl Crystals in Confinement*, Journal of Physical Chemistry Letters, 5:890–895.
- [23] CHIANESE, A., D. I. Cave, S. Matzarotta. 1986. *Solubility and Metastable Zone Width of Sodium Chloride in Water–Diethylene Glycol Mixtures*. J. Chem. Eng. Data 31:329–332.
- [24] SHAHIDZADEH-BONN, N., S. Rafai, D. Bonn, G. WEGDAM. 2008. *Salt Crystallization during Evaporation: Impact of Interfacial Properties*, Langmuir 24, 2008, 8599–8605.
- [25] SUNAGAWA, I. 1999. *Growth and Morphology of Crystals*. Forma 14:147-166.
- [26] STEIGER, M. 2005. *Growth in Porous Materials – I: the Crystallization Pressure of large crystals*. Journal of Crystal Growth, 282:455-469.